Spatiotemporal Relationships between Climate and Whitebark Pine Mortality in the Greater Yellowstone Ecosystem

Jeffrey T. Jewett, Rick L. Lawrence, Lucy A. Marshall, Paul E. Gessler, Scott L. Powell, Shannon L. Savage

Abstract: Whitebark pine (*Pinus albicaulis*) serves as a subalpine keystone species by regulating snowmelt runoff, reducing soil erosion, facilitating the growth of other plants, and providing food for wildlife. Mountain pine beetle (*Dendroctonus ponderosae*) is an ideal bioindicator of climate change, because its life cycle is temperature-dependent. Western North America is currently experiencing the largest outbreak of mountain pine beetle on record, and evidence suggests that a changing climate has accelerated the life cycle of this bark beetle. This study explored the relationships between climate, mountain pine beetles, and whitebark pine mortality in the Greater Yellowstone Ecosystem. A time series of Landsat satellite imagery (nine images) was used to monitor whitebark pine mortality in the Greater Yellowstone Ecosystem from 1999 to 2008. The patterns of mortality were analyzed with respect to monthly climate variations over the 9-year period. The impacts of topography and autocorrelation (both spatial and temporal) were also analyzed. The most important predictor variables were autocorrelation terms, indicating a strong host-tree depletion effect. Both drier and warmer climatic conditions favored increased whitebark pine mortality. These results show for the first time a statistical link between climate variability and whitebark pine mortality, probably mediated by mountain pine beetles. FOR. SCI. 57(4):320–335.

Keywords: mountain pine beetle, climate change, grizzly bears, Landsat, enhanced wetness difference index, regression tree

WHITEBARK PINE (*PINUS ALBICAULIS*) is both ecologically critical and useful as a broader environmental monitoring tool. This five-needled pine grows at the highest forested elevations of the northern Rocky Mountains of the United States, surviving conditions that are too cold, dry, and windy for other tree species. Whitebark pine is considered an ecological keystone species in the subalpine environment, where it stabilizes soil, moderates snowfall runoff, facilitates the growth of shade-tolerant tree species, and provides an unparalleled wildlife food source, especially for birds, squirrels, and bears (Tomback 2001). No other tree species in the subalpine zone provides a comparable level of ecological services. Grizzly bears (*Ursus arctos horribilis*) in the Greater Yellowstone Ecosystem (GYE) use nutrient-rich whitebark pine seeds as a critical late-summer prehibernation food source, and the availability of whitebark pine seeds is strongly connected to grizzly bear survival (Mattson et al. 1992). The seeds of whitebark pine are so important for bear survival in the GYE that whitebark pine zones are considered "critical habitat" by the federal agencies monitoring recovery of the grizzly bear from the threatened species list (Tomback et al. 2001).

Mountain pine beetle (*Dendroctonus ponderosae*) (MPB) is an ideal bioindicator of climate change (Logan and Bentz 1999). Its life cycle timing is temperature-dependent, it has the ability to reproduce rapidly in response to an increasingly suitable habitat, and a large increase in its population is easy to monitor: whole forests turn distinctively red as they are killed by the beetle. Although it is a biologically suitable host tree, historically MPBs were rare in whitebark pine, generally only affecting weak trees or having a mild outbreak during unusually warm and dry climatic periods, such as during the 1930s (Perkins and Swetnam 1996, Logan and Powell 2001).

Whitebark pine ecosystems are especially vulnerable to the effects of climate change. Slow-growing whitebark pine trees already live at the tops of mountains, making climate-induced uphill migration difficult. Models of the responses of whitebark pine to a changing climate predict a 97% loss in climatically suitable habitat by the end of the century (Warwell et al. 2006). This tree is vitally important to a diverse assortment of species yet is in peril from a variety of threats, including direct and indirect effects of climate change.

Whitebark Pine

Whitebark pine is a five-needled, high-elevation pine found near the upper tree line primarily in the northern Rocky Mountains of the United States and Canada (Wyoming, Idaho, Montana, British Columbia, and Alberta). Nearly all whitebark pine in the United States is found on federal land, almost half in national parks or designated

Jeffrey T. Jewett, Montana State University—jefftjewett@yahoo.com. Rick L. Lawrence, Montana State University, Land Resources and Environmental Science, PO Box 173490, Bozeman, MT 59717—Phone: (406) 994-5409; Fax: (406) 994-5122; rickl@montana.edu. Lucy A. Marshall, Montana State University—lmarshall@montana.edu. Paul E. Gessler—University of Idaho; paulg@uidaho.edu. Scott L. Powell, Montana State University—spowell@montana.edu. Shannon L. Savage, Montana State University—shannon.lea.savage@gmail.com.

Acknowledgments: We acknowledge the financial support provided by the Upper Midwest Aerospace Consortium. Many employees of the US Forest Service and National Park Service provided valuable data and personal expertise to guide various iterations of this project.

Manuscript received June 16 2010, accepted December 16 2010

wilderness areas (Keane 2000). Occupying 10–15% of forested land in the northern Rockies, whitebark pine grows both as a climax species and as a seral species in mixed stands (Arno and Hoff 1990), where it is often successionally replaced by the more shade-tolerant subalpine fir (*Abies lasiocarpa*) and Engelmann spruce (*Picea engelmannii*).

Arguably, the most important role whitebark pine plays in its ecosystem is as a food source for birds, bears, and small mammals. The seeds of whitebark pine are far larger and more nutritious than those of nearly any other available plant food source, and their high fat content makes the seeds exceptionally valuable as a prewinter food source (Mattson and Reinhart 1997). The importance of whitebark pine to bears, especially grizzly bears, cannot be overstated. When given an opportunity to eat whitebark pine seeds, grizzly bears will eat little else (Mattson and Reinhart 1997). In the GYE, grizzly bears obtain between 25 and 66% of their energy from whitebark pine seeds (Mattson et al. 2001).

Threats

Populations of whitebark pine have been declining for the last 90 years across its range in the northern Rockies (Kendall and Keane 2001). Whitebark pines are slow-growing and slow to reach sexual maturity, meaning that population declines will have long-lasting effects to the ecosystem (Keane 2000). Wildfire suppression has led to wide-scale successional replacement by more shade-tolerant conifers, and attacks by the invasive fungus white pine blister rust (*Cronartium ribicola*) have killed or weakened many whitebark pines (Arno 1986, Brown et al. 1994, Kendall and Keane 2001, McDonald and Hoff 2001). The GYE historically had one of the lowest rates of blister rust infection in whitebark pine because of its cold, dry climate, but a 2006 survey indicated an average infection rate of 25% across the ecosystem, double the infection rate from a decade earlier (Kendall et al. 1996, Reinhart et al. 2007). In addition to direct mortality, blister rust infection in whitebark pine leads to both preferential selection and increased infection by MPB, yielding synergistic mortality (Kendall and Keane 2001, Bockino 2007). Finally, warming global temperatures are projected to reduce suitable habitat for whitebark pine. A bioclimatic model for western North America predicts a 70% decline in suitable habitat for whitebark pine by 2030 and a 97% decline by 2100 (Warwell et al. 2006). Although blister rust is a serious threat to whitebark pine survival, blister rust generally requires more than a decade to kill a mature tree by itself, making it more of a long-term rather than imminent concern to whitebark pine populations (Kendall and Keane 2001).

Mountain Pine Beetles

The most immediate threat to whitebark pine is an epidemic of MPBs, which currently is the most widespread in at least 70 years. Climate change has been suggested as a factor contributing to this outbreak (Carroll et al. 2003). The United States had 1.6 million ha of pine infested with MPBs as of 2007, and the outbreak is even larger in Canada, where 20 million ha of pine were infested in 2007, an order of magnitude larger than any previous Canadian outbreak (Gibson et al. 2008, Kurz et al. 2008). The MPB outbreak in whitebark pine has not received the same level of attention as the outbreak in lodgepole pine (*Pinus contorta*), perhaps because 85% of this infestation is in lodgepole pine, because whitebark pine habitat is more removed from common human interaction, and also because whitebark pine is not a common timber species (Gibson et al. 2008). The US Forest Service's Aerial Detection Survey of the GYE recorded only 535 acres of MPB-infested whitebark pine in 1999, with increases nearly every year to 171,572 acres in 2007, a 320-fold increase (Gibson et al. 2008, Logan et al. 2009). Although the US Forest Service argues that similar conditions existed in the 1930s, entomologist Jesse Logan states that "Nothing comparable to what is occurring today has been observed in recorded history or exists in the disturbance legacy of this long-lived species" (Gibson et al. 2008, Logan et al. 2009).

After spending 1–3 years developing as eggs, larvae, and pupae in the host tree phloem, adult MPBs emerge in mid-summer and fly to a new host tree where eggs can be deposited to initiate the next life cycle. During an epidemic, hundreds of beetles aggregate on the same tree to form a "mass attack" that overwhelms host tree defenses. Attacked pines increase sap output in an attempt to "pitch-out" attacking beetles, but this defense is compromised by drought and overwhelmed by a beetle mass attack (Powell and Bentz 2009). Larvae of MPBs feed in the phloem of the host tree, eventually girdling it. Blue-stain fungus symbiotic with the MPB is transported by the beetle into the tree and contributes to tree death by interrupting water transport in the pine (Bentz et al. 2010). The combination of the MPB and fungus kills the tree (Amman et al. 1989, Bentz et al. 2010). Attacked trees generally begin to die within 2 weeks of attack (known as the "green-attack" or "fader" stage), and, within 1 year of the initial attack, host trees typically develop a noticeably red canopy due to dead needles (known as the "red-attack" stage) (Safranyik 2004). Within 3 years after the attack, most trees will be defoliated (known as the "gray-attack" stage) (Wulder et al. 2006a).

MPBs were historically rare in whitebark pine, because the harsh winters and cool summers common to whitebark pine zones did not provide favorable growth conditions for the beetle. MPB growth rates are largely temperature-dependent, with warmer temperatures leading to accelerated life cycles (Logan and Bentz 1999, Bentz et al. 2010). The relatively warm climate found in lodgepole pine forests allows MPBs to complete a life cycle in 1 year (known as univoltinism), whereas 2-year life cycles (known as semivoltinism) and even 3-year life cycles have historically been the standard in the cooler whitebark pine zones (Amman 1973a, Bentz et al. 2010). Life cycles longer than 1 year weaken the synchrony of adult MPB emergence, which historically have prevented MPBs from being a major presence in whitebark pine habitat (Bentz and Schen-Langenheim 2006). Mathematical models of MPB life cycles in whitebark pine zones show that an average increase in host tree phloem temperature of only 2–3° C would enable beetles to reproduce rapidly by shifting from 2- or 3-year life cycles to 1-year life cycles (Logan and Powell

2001, Powell and Logan 2005). This change in thermal habitat suitability is distinctly nonlinear: warming temperatures initially *decrease* MPB habitat suitability (by disrupting the ability of MPBs to synchronously "mass attack" host trees), until the univoltinism threshold is met, which in turn causes a rapid *increase* in habitat suitability (Logan and Powell 2001, Powell and Logan 2005). This nonlinearity yields the potential for sudden changes in beetle population dynamics resulting from gradual temperature changes.

Both past and current MPB outbreaks display evidence of being climate-influenced. A MPB outbreak in Idaho whitebark pine stands during the late 1920s and early 1930s occurred during a decade-long warming of 2.5°C above average as well as during a sustained drought (Perkins and Swetnam 1996, Logan and Powell 2001, Perkins and Roberts 2003), consistent with the Logan and Powell life cycle model. Biologists have observed current MPB outbreaks in central Idaho at whitebark pine sites above 3,000 m, where historically it was too cool for the beetles to thrive (Powell and Logan 2005). The beetles now appear able to complete a life cycle in 1 or 2 years in whitebark pine zones, whereas just 20 years ago this typically required 3 years (Amman 1973b, Bentz and Schen-Langenheim 2006, Bentz et al. 2010).

In addition to affecting growth rates, temperature is vitally important in regulating MPB populations. Cold-induced mortality is the most important factor in MPB population dynamics (Régnière and Bentz 2007). Because of the timing of cryoprotectant manufacture, MPBs can often withstand colder temperatures in mid-winter than during spring or fall (Bentz and Mullins 1999), indicating that the timing of cold snaps is perhaps as significant as the actual temperature.

The current MPB outbreak in whitebark pine threatens the vital function that whitebark pine plays in the high-mountain ecosystem, particularly as it affects grizzly bears. In 2010, the US Fish and Wildlife Service (USFWS) was forced to restore the GYE population of grizzly bears to the federal threatened species list after losing an appeal of the 2007 delisting in federal court. One of two successful claims against the USFWS in the federal lawsuit was that the USFWS "did not adequately consider the impacts of global warming and other factors on whitebark pine nuts, a grizzly food source" (Federal Register 2010). These findings echo earlier arguments by scientists dissenting the 2007 delisting, which claimed that the perilous future of whitebark pine meant that the security of the grizzly population was also threatened (Hall 2007). USFWS argued in favor of delisting the grizzly by stating "… (only) 16 percent of the total area of whitebark pine found in the GYE … has experienced some level of mortality due to mountain pine beetles" (Logan et al. 2009). Recent evidence suggests that current MPB activity is much higher than the USFWS posits, with 79% of whitebark pine zone in the GYE showing some level of canopy mortality and 27% showing "moderate" or "high" canopy mortality (Goetz et al. 2009). Warmer temperatures due to global climate change are expected to increase MPB activity in whitebark pine zones for at least an additional 30 years, according to mathematical modeling of beetle life cycles (Hicke et al. 2006). If climate change is altering the suitability of whitebark pine zones as MPB habitat, then an entire subalpine ecosystem could be at risk of collapsing, as whitebark pine is removed from the landscape and is no longer able to play the role of subalpine keystone species.

Detection with Remote Sensing and Ancillary Data

Detecting and monitoring MPB activity have been the focus of many remote sensing studies since the 1960s (Wulder et al. 2006a). Landsat is an effective tool for measuring landscape-wide changes, although it is not very sensitive to subepidemic levels of MPB infestation (Safranyik 2004, Wulder et al. 2006a). Most studies involve use of one or more derived spectral vegetation indices to distinguish "red-attack" stands. Red-attack stands are spectrally distinguishable from green vegetation through increased reflectance from 850 to 1100 nm (near-infrared) and from 600 to 700 nm (red), in addition to a decrease in green reflectance (500 to 600 nm) (Wulder et al. 2006a). These spectral response changes are caused by the loss of needle moisture followed by the destruction of photosynthetic pigments and cellular structures in the needles (Wulder et al. 2006a).

To detect subtle changes over time, such as a forest undergoing beetle attack, a multidate series of images has been shown to be more effective than a pair of images (Skakun et al. 2003, Goodwin et al. 2008). The enhanced wetness difference index (EWDI), defined as the difference in tasseled cap wetness (TC_{Wet}) for two or more dates, has been shown to be effective at detecting red-attack stands of lodgepole pine (67–78% overall accuracy), with greater accuracy in more heavily infested stands (Franklin et al. 2001, Skakun et al. 2003, Wulder et al. 2006b). TC_{Wet} is determined largely by reflectance in the middle-infrared portion of the electromagnetic spectrum (Landsat bands 5 and 7 at 1.55–1.75 and 2.08–2.35 μm, respectively) (Huang et al. 2002):

$$\begin{aligned} TC_{Wet} = {} & 0.2626(\text{Band 1}) + 0.2141(\text{Band 2}) \\ & + 0.0926(\text{Band 3}) + 0.0656(\text{Band 4}) \\ & - 0.7629(\text{Band 5}) - 0.5388(\text{Band 7}) \end{aligned}$$

Leaves with low water content reflect much more strongly in middle-infrared than moist leaves (Crist and Ciccone 1984, Carter 1991). EWDI detects red-attack stands by contrasting the canopy moisture in live vegetation with the very dry canopy of red-attack stands and has been shown to be less sensitive to topographic effects or viewing angle effects than bandwise analysis and most other vegetation indices (Cohen and Spies 1992, Song and Woodcock 2003). A decrease in TC_{Wet} over time (negative EWDI value) is the best overall indicator of conifer mortality (Collins and Woodcock 1996).

Although EWDI has been effective in detecting red-attack stands in lodgepole pine, the efficacy of this method has not previously been shown in whitebark pine. The grassy meadows and rocky outcroppings that are common in whitebark pine forests make the use of this method potentially more problematic, as changes to grasses and

shrubs will also affect EWDI values. The free archive of historical high-resolution imagery available on Google Earth (Google, Inc. 2009) allows establishment of a relationship between red-attack in whitebark pine and Landsat-derived EWDI values. Google Earth provides high-resolution coverage of the entire GYE, often over multiple dates, from sources including the Quickbird satellite (2.4-m multispectral pixels or 0.7-m pan-sharpened pixels) and aerial imagery (1-m pixels) from the National Agriculture Imagery Program. This high-resolution data set allows visual identification of individual whitebark pine trees under attack from MPB. Although perhaps not as accurate as on-the-ground field data, this method is much quicker and less expensive than actual on-the-ground field verification of forest conditions and is available for retrospective studies, while still providing acceptable verification of our statistical methods.

Environmental variables such as temperature, precipitation, and stand conditions are often linked to MPB outbreak and tend to be highly autocorrelated in both space and time (Bentz et al. 2010). To spread to a new area, a MPB outbreak requires suitable host trees, the presence of an infectious agent (emergent adult beetles), and a favorable climate for beetle development. Dispersal distance might be of importance when MPB outbreak spread is modeled, but adult MPB dispersal distance is poorly understood. Estimates indicate that short dispersal distances (less than 30 m) are more likely, but longer distances, occasionally more than 100 km, are possible (Robertson et al. 2007). The presence or absence of MPB red attack in the past is important in predicting the likelihood of its current presence or absence. The relationship between past and current MPB activity is probably nonlinear, but high levels of recent MPB activity decrease the likelihood of current attack, evidently because potential host trees have been depleted (Aukema et al. 2008, Powell and Bentz 2009). These impacts from past MPB activity are also important in adjacent areas, because host depletion effects have been noted up to 18 km away (Aukema et al. 2008). Both temperature and precipitation have been found to have an impact on MPB outbreaks, but these have previously been documented only at coarse spatial scales and never before in whitebark pine (Carroll et al. 2003, Aukema et al. 2008).

Study Objectives

We explored the connection between climate and whitebark pine mortality. MPB has been the predominant nonfire cause of whitebark pine mortality in the GYE for the last decade; therefore, evaluations of climatic impacts on whitebark pine mortality were focused on the response of MPB to changing climatic conditions. MPB life cycles are dependent on phloem temperature in their host trees (which in turn is controlled by air temperature); it was expected, therefore, that drier and warmer climatic conditions would be favorable to beetle survival, resulting in an observed increase in whitebark pine mortality (Powell and Logan 2005). A time series of Landsat imagery was used to monitor whitebark pine mortality in the GYE from 1999 to 2008. The patterns of mortality were analyzed with respect to monthly climate variations (climate anomalies) over the 10-year period. The affects of topography and autocorrelation (both spatial and temporal) were also analyzed with respect to whitebark pine mortality. Various subsets of predictor variables were combined in predictive models to best elucidate relationships among variables. Given previously modeled changes in MPB voltinism due to climate change (Logan and Powell 2001, Hicke et al. 2006), it was also predicted that toward the end of the study period (2008), climate conditions from 1 and 2 years before the image date would become relatively more important to MPB survival than they were at the beginning of the study period (2003). The use of spatially and temporally explicit climate data across an ecosystem combined with spatially and temporally explicit conifer mortality data generated from the Landsat imagery allowed the investigation, at a landscape scale, of questions regarding climate change, MPB life cycles, and whitebark pine mortality.

Methods

Overview of Methods

Nine Landsat images of the GYE from 1999 to 2008 were geometrically and radiometrically processed to a vegetation index (EWDI) suitable for detecting conifer mortality over time. Spatially explicit monthly temperature and precipitation data were compared with long-term average temperature and precipitation data to create climate anomaly data sets. A digital elevation model (DEM) was used to create slope and aspect data sets. Wildfires were a potentially confounding source of abrupt conifer mortality, so areas that experienced a wildfire during the study period were removed from the area of analysis. Climate, topographic, and conifer mortality data were extracted from approximately 40,000 randomly selected points across the study area. The data from these points were used to create and test regression tree models. Twenty-four separate regression trees were built using various subsets of predictor variables to analyze relationships between climate, topography, and the response variable EWDI, a measure of conifer mortality. These regression trees were compared with respect to the amount of data set deviance explained and analyzed for the strength and direction of variable relationships. Separate from the above analysis, high-resolution aerial and satellite imagery available on Google Earth was used to confirm the relationship between EWDI and MPB-caused red-attack stands of whitebark pine.

Study Area

The study area encompassed 345,757 ha of previously mapped (Landenburger and Lawrence 2006, Landenburger et al. 2008) whitebark pine habitat in the core of the GYE, imaged by the Landsat satellites (path 38, row 29) (Figure 1). Yellowstone National Park comprised the center of the study area, and the vast majority of the federally designated Greater Yellowstone Grizzly Bear Primary Conservation Area was included. The study area also included sections of the Gallatin, Custer, Shoshone, Bridger-Teton, and Beaverhead-Deerlodge National Forests. Elevation within

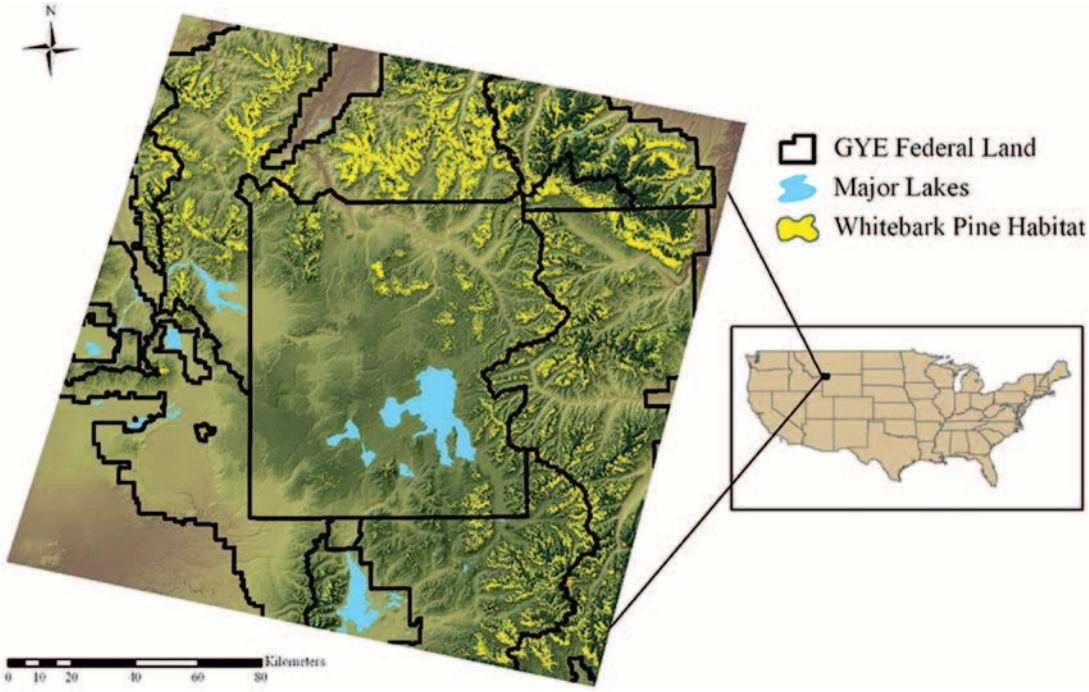

Figure 1. Study area map displayed over a shaded relief map of the GYE. Whitebark pine habitat is taken from Landenburger and Lawrence 2006.

the study area ranged from 2,410 to 3,681 m, with a mean elevation of 2,816 m. Mean January minimum temperature for whitebark pine environments throughout its range is −14°C, with an absolute minimum of −34°C. Mean July maximum temperature is 18°C, with an absolute maximum of 29°C. Yearly precipitation averages 931 mm, with 85% generally falling as snow (Weaver 1990, 1992).

The Landenburger and Lawrence map was used to restrict the study area to whitebark pine habitat because this map provided a highly accurate (95.8% accuracy) guide to whitebark pine habitat in the GYE and was mapped at the same scale as the current research (30-m pixels). One shortcoming of this map is a 20% overprediction of whitebark pine at the highest elevations (Landenburger et al. 2008). Whitebark pine grows in sparse stands at the highest elevations, including many areas with a high proportion of exposed soil. To compensate for this known issue with low-cover, high-elevation areas, the National Land Cover Database 2001 Percent Cover map (accuracy ranged from 78 to 93%) was used to further restrict the study to only those areas with greater than 0% canopy cover (Homer et al. 2004).

Analysis of Relationship between Whitebark Pine Mortality and Climate

Imagery

Near-anniversary Landsat Enhanced Thematic Mapper Plus (ETM+) and Thematic Mapper (TM) imagery (pixel size 30 × 30 m = 0.09 ha) was obtained for all years from 1999 to 2008, except for 2000, which was unavailable because of persistent cloud and smoke cover (Table 1). The 2007 and 2008 images were ETM+ imagery with the scan-line corrector (SLC) off, leaving large data gaps for those years. These gaps affect approximately 22% of the imagery, but these images were selected because ETM+ provided the highest quality imagery available for the study area for these years, the analysis was based on a sample of the data, and there was no reason to believe that the gaps biased the data. Late summer and early fall (ranging from Aug. 9 to Oct. 6) images were chosen to minimize the effects of snow, snowmelt, and understory green-up on TC_{Wet}. All images were geometrically registered to a base Landsat image (Sept. 15, 1999 ETM+) to within 0.5-pixel root mean squared error.

Climate Data

Spatially and temporally explicit climate data were obtained from the Parameter-elevation Regressions on Independent Slopes Model (PRISM) group at Oregon State University (PRISM Group and Oregon State University 2004) (Table 2). Nationwide data sets for monthly average minimum temperature (October–March), monthly average maximum temperature (April–September), 30-year-average monthly temperature (April–September: maximum, October–March: minimum), monthly average precipitation, and 30-year-average monthly precipitation were acquired in raster format. Each month's average maximum temperature values were subtracted, by pixel, from the 30-year-average monthly temperature to create temperature anomaly data sets. Each month's precipitation values were subtracted, by pixel, from the 30-year-average monthly precipitation to create precipitation anomaly data sets. Degree–day and spring precipitation anomaly data sets were created based on MPB climate suitability factors from Safranyik and colleagues (Safranyik et al. 1975, Carroll et al. 2003). The degree day data set represented cumulative temperature

Table 1. Landsat imagery used in this study

Date	Sensor	Notes
Sept. 15, 1999	ETM+	Geometric base image
Sept. 20, 2001	ETM+	Radiometric base image
Sept. 23, 2002	ETM+	
Oct. 4, 2003	TM	
Oct. 6, 2004	TM	
Sept. 7, 2005	TM	
Aug. 9, 2006	TM	
Sept. 21, 2007	ETM+	SLC off
Aug. 22, 2008	ETM+	SLC off

suitable for MPB growth. This was calculated by determining the number of degrees in excess of 5.5°C from monthly average temperatures for July, August, and September of the image year, multiplying these excesses by the number of days in the month, and then summing all 3 months. The spring precipitation anomalies were computed as the sum of the precipitation anomalies for April, May, and June for the image year and 1 year prior. The nationwide climate data sets were clipped to the study area. All climate data sets were resampled to 30-m pixels for analysis.

Ancillary Data

A DEM was obtained from the National Elevation Dataset at 30-m horizontal resolution (US Geological Survey 2009). The DEM was used to create slope and aspect data sets using a 3 × 3 moving window (90 m × 90 m) applied to the DEM. Aspect was binned into a 9-value factor data set, representing north, northeast, east, southeast, south, southwest, west, northwest, and flat.

Perimeters of wildfires in the study area were obtained from three sources: US Forest Service Region 1 Fire History Layer (Smail and Tanke 2008), Yellowstone National Park Fire History Layer (Spatial Analysis Center 2005), and the federal Landscape Fire and Resource Management Planning Tools Project (LANDFIRE) Rapid Refresh product, which is derived from MODIS satellite imagery (LANDFIRE 2007). These three fire history data sets were rasterized to 30-m pixels and combined so that a fire recorded in any layer resulted in a fire in the combined raster. Fire perimeters were separately calculated for each individual year, 1999–2008. Cumulative fire history masks were created for each year of imagery (i.e., the 2005 fire mask included fires from 1999, 2000, 2001, 2002, 2003, 2004, and 2005, whereas the 2004 mask did not include 2005 fires).

Image Processing

All images were converted to top-of-atmosphere reflectance, which has been shown to partially compensate for atmospheric and illumination differences between scenes

Table 2. Climate data sets

Climate data set	Dates	Variable abbreviations	Native spatial resolution (m)
Maximum temperature (monthly average)	4/2000–9/2007, Apr.–Sept. (summer)		4,000
Minimum temperature (monthly average)	10/1999–3/2007, Oct.–Mar. (winter)		4,000
Minimum temperature anomaly (monthly)	4/2000–9/2007, Apr.–Sept. (summer)	ano_{Y-X}Oct, ano_{Y-X}Nov, ano_{Y-X}Dec, ano_{Y-X}Jan, ano_{Y-X}Feb, ano_{Y-X}Mar	4,000
Maximum temperature anomaly (monthly)	10/1999–3/2007, Oct.–Mar. (winter)	ano_{Y-X}Apr, ano_{Y-X}May, ano_{Y-X}Jun, ano_{Y-X}Jul, ano_{Y-X}Aug, ano_{Y-X}Sep	4,000
1971–2000 average maximum temperature (monthly)	Apr.–Sept. (summer)	avgApr, avgMay, avgJun, avgJul, avgAug, avgSep	800
1971–2000 Average minimum temperature (monthly)	Oct.–Mar. (winter)	avgOct, avgNov, avgDec, avgJan, avgFeb, avgMar	800
Summer temperature anomaly	Apr.–Sept. (summer)	$_{Y-X}$sum	4,000
Winter temperature anomaly	Oct.–Mar. (winter)	$_{Y-X}$win	4,000
Degree days		degday	4,000
Precipitation (monthly average)	10/1999–6/2008, Jan.–Dec.	—	4,000
Precipitation anomaly (monthly)	Jan.–Dec.	pan_{Y-X}Jan, pan_{Y-X}Feb, pan_{Y-X}Mar, pan_{Y-X}Apr, pan_{Y-X}May, pan_{Y-X}Jun, pan_{Y-X}Jul, pan_{Y-X}Aug, pan_{Y-X}Sep, pan_{Y-X}Oct, pan_{Y-X}Nov, pan_{Y-X}Dec	4,000
Water–year precipitation anomaly	Oct.–September	$_{Y-X}$wtryr	4,000
Spring precipitation anomaly	Apr.–June	spr-pano	4,000
1971–2000 Average precipitation (monthly)	Jan.–Dec.	pavgJan, pavgFeb, pavgMar, pavgApr, pavgMay, pavgJun, pavgJul, pavgAug, pavgSep, pavgOct, pavgNov, pavgDec	800

Y indicates the year of the satellite image, and X indicates the number of years before the image year. For example, pan_{Y-X}Jan represents pan_{Y-0}Jan, pan_{Y-1}Jan, pan_{Y-2}Jan, and pan_{Y-3}Jan. The variable pan_{Y-2}Jan would indicate the precipitation anomaly from January for 2 years before the date of the imagery.

(Huang et al. 2001). Absolute normalization involves converting a radiometric base image to surface reflectance, followed by matching all other images to the radiometric base image via regression-based normalizations. The absolute-normalization procedure has been shown to provide the best radiometric normalization for multidate imagery (Schroeder et al. 2006). Dark object subtraction (DOS) was used to provide the first half of the absolute-normalization process, an absolute atmospheric correction to surface reflectance for the radiometric base image (Sept. 20, 2001 ETM+). DOS effectively removes atmospheric effects in TC_{Wet} (Song and Woodcock 2003). Cloud, smoke, and snow masking on all images was performed using manual digitizing. From 2003 to 2006, cloud, smoke, and snow masking removed no more than 13.4% of the study area from any one image. The SLC-off data gaps in the 2007 and 2008 ETM+ images caused more portions of the study area to be removed for those years (18.7 and 23.5%, respectively).

A tasseled cap transformation was performed using Huang's ETM+ coefficients (Huang et al. 2002). For the second half of the absolute-normalization procedure, TC_{Wet} components were normalized to the absolutely corrected radiometric base image wetness using pseudoinvariant targets to build normalization regression equations. Paired *t* tests comparing both the fitted points and the uncorrected points with the 2001 radiometric base image showed that the regression (fitted points) improved the match for all dates except 2003 ($P < 0.001$). Despite having $P = 0.2285$, the regression-based correction for the 2003 image was used because it reduced the sum of squared errors by 62% from that for the uncorrected image, indicating that the interdate variation was being reduced with the regression. All images were clipped to intersecting areas only, excepting the data gaps in the SLC-off images. The images were further masked to areas mapped as whitebark pine by Landenburger and Lawrence (2006).

Areas that experienced a wildfire between the base year (1999) and the image date were removed from analysis, using the fire history masks. Extensive logging was an unlikely source of substantial forest change because the majority of the study area was relatively inaccessible, high-elevation terrain and because two-thirds of GYE whitebark pine was found in protected designated wilderness areas or national parks (Logan et al. 2009). Although blister rust was present in the study area, it kills over decadal time periods and so was unlikely to cause detectable changes in EWDI over a yearly basis, especially when one is looking at 30-m pixels that would have many trees in one pixel (Tomback et al. 2001). With wildfires removed, logging unlikely, and change due to blister rust probably too slow to be detectable, we assumed that the only likely source of widespread and substantial decreases in EWDI in the study area was pine mortality from MPB attacks.

EWDI was calculated for each date versus the initial year (EWDI-to-99), as well as for each date versus the previous year (EWDI-yearly). 1999 was chosen as the initial year because it was before the current MPB epidemic began in the GYE. Spatial autocorrelation terms were created by using circular moving windows of various radii to calculate average neighborhood values of EWDI-to-99 and EWDI-yearly. The window sizes were chosen to encompass what is known (and not known) about MPB dispersal distances and extended 30, 90, and 150 m from the edge of the center pixel, which was excluded from the window (Robertson et al. 2007). An additional temporal autocorrelation term was generated (minEWDI99) to measure the minimum EWDI-to-99 value at that pixel for all years before the image date. This term measures the maximum recent impact of MPB on that pixel, to offset possible increases in TC_{Wet} caused by recently-exposed understory vegetation under a dead canopy (Table 3).

Data Extraction and Compilation

For each year from 2003 to 2008, a different set of 10,000 random points was generated. Using a different set of points for each year allowed locations that were obscured by clouds/smoke/snow in 1 year but not in others to still be included in the analysis, maximizing the area of study. These random points were used to extract the pixel value for all variables for that year. Data points for which any variable contained missing data (null) were removed from the analysis. Points at which the NLCD forest canopy cover equaled zero (nonforested) were also removed from the analysis, leaving 40,639 total points for analysis. All years from 2003 to 2008 were treated equally in the analysis. For example, for the variable "$ano_{Y\text{-}3}$Feb" (representing the temperature anomalies from the February 3 years before the image date), these temperature anomalies would come from 2005 climate data for the 2008 image, but from 2000 climate data for the 2003 image. Likewise, the EWDI data set came from a compilation of year-over-year changes from 2003 through 2008. One-third of the points were randomly selected and used to create a validation data set ($n = 13{,}527$), which was not used in building regression

Table 3. Autocorrelative predictor variables used

Autocorrelation Term	Definition
$EWDI_{Y\text{-}1}$	EWDI-yearly for the same pixel 1 yr before the image
$EWDI_{Y\text{-}2}$to99	EWDI-to-99 value from 2 yr before the image
$3x3_{Y\text{-}1}$	Average of EWDI-yearly in 30 m neighborhood from 1 yr before the image
$7x7_{Y\text{-}1}$	Average of EWDI-yearly in 90 m neighborhood from 1 yr before the image
$11x11_{Y\text{-}1}$	Average of EWDI-yearly in 150 m neighborhood from 1 yr before the image
$3x3to99_{Y\text{-}2}$	Average of EWDI-to-99 value in 30 m neighborhood from 2 yr before the image
$7x7to99_{Y\text{-}2}$	Average of EWDI-to-99 value in 90 m neighborhood from 2 yr before the image
$11x11to99_{Y\text{-}2}$	Average of EWDI-to-99 value in 150 m neighborhood from 2 yr before the image
minEWDI99	Minimum EWDI-to-99 value from all years before image

trees. The remaining two-thirds of the data points (n = 27,112) formed a training data set used to build regression trees to model the relationship between climate and whitebark pine mortality. Exploratory scatter plots and correlations between the response variable (EWDI-yearly) and various subsets of predictor variables were examined.

Regression Tree Analysis

This analysis used regression trees containing climatic, topographic, and autocorrelation variables to predict EWDI. In this way the connections between climate and whitebark pine mortality across the GYE were investigated. Regression trees were chosen for the analysis because they are nonparametric in nature, handle nonlinear data sets, and can automatically select the most useful predictor variables from a suite of reasonable predictor variables (Lawrence and Wright 2001, Rogan et al. 2003). Trees were pruned both to avoid overfitting and to simplify them to allow interpretation of the splits for ecological significance. Ten-fold cross-validation of tree residual deviance was used to inform the tree-pruning process.

Twenty-four regression trees were built using different subsets of the available predictor variables to examine different potential relationships with EWDI. All predictor variables were included in the first tree to determine whether any statistical relationship existed. The predictor variables (especially the climate terms) were highly correlated, so subsequent regression trees were built from a variety of variable subsets in an attempt to avoid ecologically spurious conclusions. For example, if the only winter temperature variable included in a regression tree was a February temperature anomaly, would a different tree that used December or January temperature perform nearly as well, indicating that "winter temperature" was really the ecologically important consideration, more so than February in particular? All climate terms were used to investigate whether whitebark pine mortality could be predicted solely on the basis of recent climate. Because of the large number of climate terms (120), another regression tree was built using only the 12 seasonal climate summary terms in an attempt to predict mortality with a smaller suite of climate variables. Regression trees were built using only temperature data and only precipitation data to further investigate climatic relationships. Topographic variables have been suggested as important factors in insect outbreaks (Perkins and Roberts 2003), especially because they have an impact on incident solar radiation, so a regression tree was built solely from slope, aspect, and elevation. The autocorrelation terms were used to build a regression tree in an attempt to better understand the effect of prior MPB attack and the neighborhood autocorrelation terms by themselves were used in another regression tree to investigate MPB dispersal. To better understand potential changes in MPB voltinism, three regression trees were built using only climate data from 1 year before the image (Y-1), 2 years before the image (Y-2), and 3 years before the image (Y-3), respectively. These trees did not have 30-year-average climate data included. Finally, regression trees were built (with and without autocorrelation terms) for each year (2003–2008) of data to investigate potential changes in the impact of climate on whitebark pine mortality during the course of the study period.

Table 4. Summary statistics comparing Landsat EWDI response between green, red-attack, and gray-attack stands of whitebark pine

	Green stands EWDI (n = 195)	Red-attack stands EWDI (n = 43)	Gray-attack stands EWDI (n = 8)
Mean	−21.4	−46.7	87.9
Median	−8	−55	71
Maximum	608	62	260
Minimum	−965	−140	−28

After each regression tree was built and pruned, the tree was used to predict EWDI values from the independent validation data set. These predicted EWDI values were compared with the observed EWDI values, generating a sum of squared errors (SSE). The total deviance in the validation data set EWDI values was calculated (total sum of squares [SST]). The SSE was subtracted from the SST and then divided by the SST to provide a measure of total data set deviance explained (DDE) by the regression tree, a value analogous to R^2 in a linear regression model.

A partial DDE was calculated for each binary split to evaluate the relative importance of each variable in the regression tree. This was done by calculating the amount of deviance reduced by that split and then dividing this reduction by the root deviance. All partial DDE values for that variable were summed if a variable was used in more than one split per tree. To better understand the contribution of each variable in the tree, a relative partial DDE value was calculated (partial DDE_{Rel}). Partial DDE_{Rel} was calculated by dividing the amount of deviance explained by each variable by the total DDE for the regression tree, as opposed to the root deviance as in the standard DDE value. Partial DDE for a tree will sum to total DDE for that tree, and partial DDE_{Rel} for any tree will sum to 1.

Google Earth-Based Evaluation of EWDI Response to Red-Attack

High-resolution aerial and satellite imagery available in Google Earth was used evaluate the relationship between Landsat-derived EWDI values and visible MPB-affected red-attack stands of whitebark pine. Versions 5.0 and later of Google Earth provide the exact date of satellite image capture, and for many places on the globe multiple dates of imagery for each location are available, making time-series analysis possible. Locations were randomly generated across the study area (n = 238), stratified by the 2006 EWDI values. Stratification was done using the 2006 EWDI values because this year contained a large range of EWDI values and was the most recent image without the data gaps from Landsat SLC failure. All locations were identified in Google Earth, and the high-resolution imagery was used to classify the 30-m radius area around each point as green, red-attack, or gray-attack for each year in which suitable high-resolution imagery was available. Thirty-five locations had high-resolution imagery available for multiple years

Table 5. Summary of regression trees using yearly subsets of data points, using all predictor variables, showing explanatory terms used in each tree

Year	Validation DDE	Root variance ($\times 10^4$)	Temperature terms	Precipitation terms	Topographic terms
2003	0.1230	1,127	ano_{Y-2}Dec; avg30Nov		
2004	0.1930	1,457	ano_{Y-1}Jun; ano_{Y-4}Oct; avg30Oct		Aspect; slope
2005	0.2718	4,619			
2006	0.0900	3,512	ano_{Y-3}Feb; ano_{Y-2}Jul; avg30Feb		Slope
2007	0.6498	8,715			
2008	0.3739	2,149	avg30Oct; avg30Dec		Aspect

during the study period. These classifications were compared with Landsat-derived EWDI values for the appropriate year to determine whether EWDI was an effective measure of the presence or absence of red-attack in whitebark pine.

Results

Evaluation of EWDI Response to Red-Attack

Green (either not attacked by MPB or recently attacked but still green) stands of whitebark pine, as determined using Google Earth imagery, had a higher EWDI value than red-attack stands when both mean and median values were compared (Table 4). Gray-attack stands had much higher EWDI values than either green stands or red-attack stands, although the sample size ($n = 8$) was very low for gray-attack stands. The range of EWDI values in green stands (1,573) was also much greater than the range for red-attack (202) or gray-attack stands (288).

Landsat Analysis

No clear pattern to the DDE values for each yearly regression tree existed (Table 5), although they cannot be *directly* compared because they were based on different data sets. There is also no clear pattern to which variables were included in each yearly tree. Yearly regression trees from only climate data demonstrate the same lack of distinct patterns (Table 6). In addition, the DDE values are generally low with the exception of 2007.

The highly stochastic nature of the ecological processes being predicted yields DDE values far less than 1. The full 22-node tree had a DDE value of 0.3865 (Table 7). Most climate variables included in this tree were from 3 years before the date of imagery (measured in the October–September growing season years to match MPB life cycles). Climate terms from one, two, and three growing seasons before the image date are included in the all-climate tree (DDE = 0.1538). In both the full tree and the all-climate tree, only one summer climate variable was included (ano_{Y-1}Jul) of 20 climate variables used between the two trees. The seasonal climate summary tree (DDE = 0.1419) was almost as successful as the climate tree, using fewer predictor variables (9 versus 14) and far fewer potential predictor variables (12 versus 120). The autocorrelation tree (DDE = 0.3123) was able to explain 81% as much variation as the full 22-node tree did. It did not incorporate any of the spatial autocorrelation terms, only the temporal ones. Despite this, the tree built only on spatial autocorrelation terms (DDE = 0.1996) still performed better than any tree that did not include any autocorrelation terms. The 3×3 window (90 m across), 7×7 window (210 m across), and 11×11 window (330 m across) autocorrelation terms were all included in the tree. No topographic variables were included in any tree multiyear except the tree that only used topographic variables, which had a DDE value of 0.0015. Finally, for the trees that evaluated climate data from different growing season years, there was an increase from Y-1 (DDE = 0.1160) to Y-2 (DDE = 0.1414) to Y-3 (DDE = 0.1547).

Most of the 10 variables in the tree could be assigned a direction of relationship (positive or negative) with the response variable, EWDI (Table 8). A positive relationship existed for precipitation anomalies pan_{Y-4}Oct and pan_{Y-1}Oct, in addition to temperature anomaly ano_{Y-3}Mar. A negative relationship was demonstrated for EWDI with autocorrelation terms $EWDI_{Y-1}$, minEWDI99, $3x3to99_{Y-2}$, and $EWDI_{Y-2}$to99, in addition to temperature anomaly ano_{Y-4}Nov. The direction of the relationships for ano_{Y-4}Oct and ano_{Y-3}Feb could not be determined.

Eight of the 14 variables in the climate-only tree could be assigned a direction of correlation (positive or negative) to EWDI (Table 9). Precipitation anomaly variables pan_{Y-1}Oct and pan_{Y-2}Sep had a positive correlation with EWDI. Precipitation anomaly pan_{Y-2}Dec, long-term average December

Table 6. Summary of regression trees using yearly subsets of data points, using climate predictor variables only, showing explanatory terms used in each tree

Year	DDE validation	Root variance ($\times$ 10,000)	Temperature terms
2003	0.0081	1,127	ano_{Y-2}Dec
2004	0.0084	1,457	avg30Jan; ano_{Y-1}Feb; avg30Aug; avg30Apr
2005	0.0698	4,619	ano_{Y-2}Oct; ano_{Y-1}Mar; ano_{Y-2}Feb; ano_{Y-2}Jan; avg30Jun; avg30Feb; ano_{Y-1}Jun; ano_{Y-1}Apr; avg30Oct; ano_{Y-2}Dec
2006	0.0031	3,512	ano_{Y-4}Oct
2007	0.1755	8,715	avg30Aug; $_{Y-3}$wtryr; ano_{Y-1}Feb; ano_{Y-2}Aug; $_{Y-2}$sum
2008	0.0305	2,149	ano_{Y-1}Mar

Table 7. Summary of DDE and variables included in all regression trees, showing explanatory terms used in each tree

Model	DDE validation	Temperature terms	Precipitation terms	Topographic terms	Autocorrelation terms
Full	0.3865	ano_{Y-4}Oct; ano_{Y-3}Feb; ano_{Y-3}Mar; ano_{Y-4}Nov	pan_{Y-4}Dec; pan_{Y-1}Oct		$EWDI_{Y-1}$; minEWDI99; $3x3to99_{Y-2}$; $EWDI_{Y-2}$to99
All climate	0.1538	ano_{Y-3}Feb; ano_{Y-2}Mar; avg30Dec; anoY-1Mar; anoY-1Apr; anoY-2Dec; anoY-1Jul; anoY-3Apr	pan_{Y-3}Sep; panY-1May; panY-1Oct; panY-2Dec; panY-4Oct; panY-2Sep		
Seasonal climate summary	0.1419	$_{Y-3}$win; $_{Y-1}$win; $_{Y-2}$win; $_{Y-1}$sum	$_{Y-3}$wtryr; $_{Y-1}$wtryr; spr-pano; $_{Y-2}$wtryr; $_{Y-0}$wtryr		
Autocorrelation	0.3123				$ewdi_{Y-1}$; minEWDI99; $ewdi_{Y-2}$to99
Spatial autocorrelation only	0.1996				$3x3_{Y-1}$; $11x11_{Y-1}$; $3x3to99_{Y-2}$; $7x7_{Y-1}$
Topographic effects	0.0015			Aspect; slope	
Temperature	0.1505	ano_{Y-3}Feb; ano_{Y-2}Mar; Avg30Dec; ano_{Y-1}Mar; ano_{Y-1}Apr; ano_{Y-2}Dec; ano_{Y-2}Feb; ano_{Y-3}Sep; ano_{Y-2}Oct; ano_{Y-3}Jun; ano_{Y-3}Jan; ano_{Y-1}Sep; ano_{Y-3}Apr			
Precipitation	0.1482	pan_{Y-4}Dec; pan_{Y-2}Jan; panYMar; pan_{Y-1}Aug; pan_{Y-3}Oct; panYApr; pan_{Y-2}Sep; pavgMay; pan_{Y-3}Nov pavgMar; pan_{Y-2}Dec pan_{Y-3}Feb; pan_{Y-1}Nov; pavgJun; pan_{Y-3}Mar			
Y-1 climate	0.1160	ano_{Y-1}Mar; ano_{Y-1}Sep; ano_{Y-2}Oct; ano_{Y-1}Apr	pan_{Y-2}Nov; pan_{Y-1}Sep; pan_{Y-1}Aug; pan_{Y-1}Jun; pan_{Y-1}Jan		
Y-2 climate	0.1414	anoY-2Mar; ano_{Y-3}Nov; ano_{Y-2}Sep; ano_{Y-2}Feb; ano_{Y-2}Apr; ano_{Y-3}Dec	pan_{Y-2}Jan; pan_{Y-2}Sep; pan_{Y-2}Mar; pan_{Y-2}Feb; pan_{Y-2}Apr; pan_{Y-2}Aug;		
Y-3 climate	0.1547	ano_{Y-3}Feb; $_{Y-3}$win; ano_{Y-3}Sep; ano_{Y-4}Nov; ano_{Y-3}Mar; ano_{Y-3}Apr; ano_{Y-3}Aug	pan_{Y-3}Mar; pan_{Y-3}Sep; pan_{Y-4}Oct; pan_{Y-3}Jun		

Table 8. Interpretation of predictor variable relationships with response variable EWDI for 22-node final full-variable regression tree

Variable	Type of variable	Response direction with EWDI	Supports expectation?
ano_{Y-4}Nov	Temperature	Negative	E1
pan_{Y-4}Oct	Precipitation	Positive	E2
pan_{Y-1}Oct	Precipitation	Positive	E2
$EWDI_{Y-1}$	Autocorrelation	Negative	E3
minEWDI99	Autocorrelation	Negative	E3
$3x3to99_{Y-2}$	Autocorrelation	Negative	E3
$EWDI_{Y-2}$to99	Autocorrelation	Negative	E3
ano_{Y-3}Mar	Temperature	Positive	No
ano_{Y-3}Feb	Temperature	Not Clear	NA
ano_{Y-4}Oct	Temperature	Not Clear	NA

Explanation of expectations: E1, warmer temperatures decrease MPB mortality and/or increase MPB growth rates, leading to an increase in whitebark pine mortality and then to a decrease in EWDI values; E2, drier conditions reduce ability of whitebark pine to repel attacks by MPB, leading to an increase in whitebark pine mortality and then to a decrease in EWDI values; E3, previous MPB activity in a cell or neighboring cell decreases the likelihood of current MPB activity, because of depletion of potential host trees, leading to an increase in EWDI; No, does not support either expectation 1, expectation 2, or expectation 3; NA, not applicable, because of lack of interpretability of variable relationship.

temperature (Avg30Dec), and temperature anomalies ano_{Y-1}Mar, ano_{Y-2}Dec, ano_{Y-1}Jul, and ano_{Y-3}Apr all showed a negative correlation with EWDI. The direction of correlation for the following six variables could not be determined, given the nature of the regression tree: ano_{Y-3}Feb, ano_{Y-2}Mar, ano_{Y-1}Apr, pan_{Y-3}Sep, pan_{Y-1}May, and pan_{Y-4}Oct.

For the all-variable tree, $EWDI_{Y-1}$ was by far the most important variable, followed by minEWDI99 (Table 10). Taken together, these two autocorrelation terms accounted for more than 71% of the data set variation explained (DDE_{Rel}) of the data set variation explained, whereas the next most important term (ano_{Y-3}Feb) accounted for only 9% of DDE_{Rel}. The autocorrelation variables were used frequently and accounted for more than half of the splits in the regression tree. Climate variables from the Y-3 growth

Table 9. Interpretation of predictor variable relationships with response variable EWDI for 17-node climate variables only regression tree

Variable	Type of variable	Response direction with EWDI	Supports expectations?
avg30Dec	Average temperature	Negative	E1
ano_{Y-1}Mar	Temperature	Negative	E1
ano_{Y-2}Dec	Temperature	Negative	E1
ano_{Y-1}Jul	Temperature	Negative	E1
ano_{Y-3}Apr	Temperature	Negative	E1
pan_{Y-1}Oct	Precipitation	Positive	E2
pan_{Y-2}Sep	Precipitation	Positive	E2
pan_{Y-2}Dec	Precipitation	Negative	No
ano_{Y-3}Feb	Temperature	Not clear	NA
ano_{Y-2}Mar	Temperature	Not clear	NA
ano_{Y-1}Apr	Temperature	Not clear	NA
pan_{Y-3}Sep	Precipitation	Not clear	NA
pan_{Y-1}May	Precipitation	Not clear	NA
pan_{Y-4}Oct	Precipitation	Not clear	NA

Explanation of expectations: E1, warmer temperatures decrease MPB mortality and/or increase MPB growth rates, leading to an increase in whitebark pine mortality and then to a decrease in EWDI values; E2, drier conditions reduce ability of whitebark pine to repel attacks by MPB, leading to an increase in whitebark pine mortality and then to a decrease in EWDI values; No, does not support either expectation 1 or expectation 2; NA, not applicable, because of lack of interpretability of variable relationship.

Table 10. Analysis of data set variation explained, by variable, in final, all-variable, 22-node regression tree

Variable	Growth year (Oct.–Sept.)	Variable type	Partial DDE	No. splits	Partial DDE_{Rel}
$ewdi_{Y-1}$	NA	Autocorrelation	0.1792	8	0.4368
minEWDI99	NA	Autocorrelation	0.1153	3	0.2811
pan_{Y-4}Dec	Y-3	Precipitation	0.0330	1	0.0805
ano_{Y-4}Oct	Y-3	Temperature	0.0087	1	0.0213
$3x3to99_{Y-2}$	NA	Autocorrelation	0.0113	2	0.0274
ano_{Y-3}Feb	Y-3	Temperature	0.0367	1	0.0895
ano_{Y-3}Mar	Y-3	Temperature	0.0122	1	0.0298
ano_{Y-4}Nov	Y-3	Temperature	0.0031	1	0.0076
$ewdi_{Y-2}$to99	NA	Autocorrelation	0.0074	2	0.0181
pan_{Y-1}Oct	Y-0	Precipitation	0.0033	1	0.0079
Total			0.4102		1.000

NA, not applicable.

year (October Y-4 to September Y-3) accounted for a partial DDE_{Rel} of 0.2287, whereas all other growth years were represented entirely by panY-1Oct, with a DDE_{Rel} of 0.0079.

In the climate-only regression tree, the most important variable was ano_{Y-3}Feb, with a partial DDE of 0.0635 (DDE_{Rel} = 0.34), but if this partial DDE is compared with the most important variable in the full tree ($EWDI_{Y-1}$, DDE = 0.1792), it explained roughly only one-third as much of the variation (Table 11). Evaluating the impact of climate variables by growth year shows substantially more importance from the Y-3 growth year than from any other.

Table 11. Analysis of data set variation explained, by variable, in climate-only, 17-node regression tree

Variable	Growth year (Oct–Sep)	Variable type	Partial DDE	No. splits	Partial DDE_{Rel}
ano_{Y-3}Feb	Y-3	Temperature	0.0635	1	0.3401
ano_{Y-2}Mar	Y-2	Temperature	0.0078	1	0.0416
avg30Dec	NA	Average temperature	0.0043	1	0.0228
ano_{Y-1}Mar	Y-1	Temperature	0.0039	1	0.0208
ano_{Y-1}Apr	Y-1	Temperature	0.0043	1	0.0228
ano_{Y-2}Dec	Y-1	Temperature	0.0157	2	0.0842
pan_{Y-3}Sep	Y-2	Precipitation	0.0206	1	0.1101
pan_{Y-1}May	Y-1	Precipitation	0.0067	1	0.0357
pan_{Y-1}Oct	Y-0	Precipitation	0.0036	1	0.0192
pan_{Y-2}Dec	Y-1	Precipitation	0.0026	1	0.0140
pan_{Y-4}Oct	Y-3	Precipitation	0.0033	1	0.0179
ano_{Y-1}Jul	Y-1	Temperature	0.0058	1	0.0309
ano_{Y-3}Apr	Y-3	Temperature	0.0379	2	0.2030
pan_{Y-2}Sep	Y-1	Precipitation	0.0069	1	0.0367
Total			0.1867		1.000

NA, not applicable.

Partial DDE_{Rel} were summed by growth year to indicate the relative importance of each growth year: Y-0 growth year (only precipitation variables included) = 0.0192, Y-1 growth year = 0.2451, Y-2 growth year = 0.1517, and Y-3 growth year = 0.5610. Temperature variables account for nearly three-quarters of explained variation in the climate-only tree.

The overall trend in EWDI study areawide progressed from low whitebark pine mortality (highly positive EWDI values) in 2003 and changing to much higher mortality (negative EWDI values) in 2004, 2005, and 2006. Low conifer mortality was observed in 2007 (positive EWDI). 2008 had more mortality, especially in the northwest portion of the study area (Gallatin National Forest) with many extremely negative EWDI values indicative of high rates of whitebark pine mortality.

Discussion

Evaluation of EWDI Response to Red-Attack Using Google Earth

In the high-resolution red-attack analysis, stands of green whitebark pine trees covered the widest spectrum of EWDI values, from very negative to very positive. Red-attack stands also covered a spectrum of values but were concentrated more on negative values. Gray-attack stands had generally positive EWDI values. These results corroborate other studies that show a relationship between MPB red-attack levels and EWDI values (Franklin et al. 2001, Skakun et al. 2003, Wulder et al. 2006b). More negative EWDI values are generally found with MPB red-attack stands. Although the sample size of gray-attack stands was too small for strong conclusions, the results do support the hypothesis that positive EWDI values can occur after the MPB stage as a result of the exposure of the forest understory when needles fall off dead trees.

Regression Tree Analysis of Landsat and Climate Data

Yearly decreases in tasseled cap wetness (EWDI) in conifer forests are indicative of conifer mortality. With use of a regression tree of only past climate anomalies and autocorrelation terms as predictor variables, mortality in whitebark pine habitat (measured by EWDI) was predicted, with 38% of the data set deviance explained. By sole use of climate terms, 15% of the deviance in the data set was explained. Assuming that MPBs were a primary cause of whitebark pine mortality during this study period allows these results to illuminate MPB population dynamics. These results support and expand on previous field studies and mathematical models that indicate climatic drivers for shifts in MPB range and life cycle. A deeper analysis of the relationships indicated by these results can inform the understanding of the future of both MPBs and whitebark pine in the GYE.

Topographic Variable Analysis

Topographic data were not included in any regression tree model, which was an unexpected result because of the microclimatic effects of slope and aspect, but this result might have been a function of the topographic effects occurring at finer scales than that of the available DEM. This finding does corroborate earlier analysis of the last major MPB outbreak in whitebark pine (during the 1930s), which also did not find topographic effects to be significant in predicting whitebark pine mortality (Perkins and Roberts 2003). The use of EWDI as a response variable also might have contributed to this finding, because vegetation indices have been found to normalize reflectance values in vegetation cover due to topographic differences (Song and Woodcock 2003). A study of an Idaho coniferous forest found that the Normalized Difference Vegetation Index with a middle-infrared-based correction for canopy closure better predicted leaf area index than a model that combined that index with elevation and/or solar insolation (solar insolation served a similar predictive function as slope and aspect did in the study reported here) (Pocewicz et al. 2004).

Autocorrelation Variable Analysis

Autocorrelation terms were very important to these models in predicting yearly changes in EWDI. Seventy-six percent of the data set deviance that could be explained (DDE_{Rel}) was explained by autocorrelation terms. All four autocorrelation terms in the full model supported the expectation that there was a clear negative correlation between EWDI and any version of EWDI from prior years ($EWDI_{Y-1}$ most strongly, but also minEWDI99, $3x3to99_{Y-2}$, and $EWDI_{Y-2}to99$). This is strong support for the third expectation (E3) from Table 8, that previous MPB activity in a cell or neighboring cell decreases the likelihood of current MPB activity, leading to an increase in EWDI (negative correlation). This negative correlation suggests that host tree depletion was more of a factor than availability of MPB in nearby pine trees for expanding the infestation, which would have given a positive correlation between EWDI and $EWDI_{Y-1}$. After a highly negative EWDI reading, positive EWDI values were expected in the future. Whitebark pine canopy is unlikely to recover on the time scale of this analysis (10 years), so this response might be due to exposing the understory grasses and shrubs to the satellite sensor after the needles fall off the whitebark pine in the gray-attack stage. The question of MPB dispersal distance is not well understood, and this study cannot shed much additional light on it. In the spatial-autocorrelation-terms-only regression tree, terms at all three distances (30, 90, and 150 m) were included in the tree, indicating that there is a dispersal effect at all three distances.

Climate Variable Analysis

Evaluating the regression trees built on climate data from different growth years can inform questions of MPB voltinism in the whitebark pine zone. MPB historically required 3-year life cycles in whitebark pine habitat, but recent field evidence suggests a shift to semivoltinism and even univoltinism (Bentz and Schen-Langenheim 2006). Comparing the different growth-year regression trees, the Y-3 climate tree explained the most data set deviance (DDE = 0.1547),

whereas the Y-1 climate tree explained the least (DDE = 0.1160). When the variables included in the full tree were evaluated, five of six climate variables were from the Y-3 growth year, and the sixth term accounted for less than 1% of the deviance explained. These results indicate that a substantial portion of the MPB population in GYE whitebark pine are still on a 3-year life cycle. On the other hand, when the climate-only tree was evaluated, the Y-1 and Y-2 growth years accounted for 0.25 and 0.15 of the deviance explained (DDE_{Rel}). This could mean that one or both of the following is true: *some* populations of MPBs in GYE whitebark pine are becoming semi- or univoltine, or climate variations experienced by 3-year life-cycle MPB populations in their second and third years of development affect MPB survival.

Temperature variables make up between 63 and 74% of the total contribution from climate variables in explaining data set deviance. The first expectation (E1 in Table 9) was that warmer temperatures (positive temperature anomalies) decrease MPB mortality and/or increase MPB growth rates, leading to an increase in whitebark pine mortality and in turn to a decrease in EWDI values. Therefore, a negative correlation between temperature anomalies and EWDI values would support this first expectation. In the full-variable tree, one temperature variable supports E1, one does not support E1, and two are unclear. Although that is not a resounding endorsement of the expectation that warmer temperatures yield increased whitebark pine mortality, the climate-only tree provides stronger evidence in support of this expectation. In the climate-only regression tree, five temperature variables support E1, none contradict it, and three are unclear. This is much stronger support. The second expectation (E2) states that drier conditions (negative precipitation anomaly) reduce the ability of whitebark pine to defend itself against attacks by MPBs, leading to an increase in whitebark pine mortality and thus to a decrease in EWDI values (positive correlation). In the full-variable tree, two precipitation variables support E2, whereas none are unclear or contradict it. For the climate-only tree, two precipitation variables support E2, one contradicts it, and three are unclear. Combining the evidence from these two trees leads to weak support of the second expectation that drier conditions lead to increased whitebark pine mortality, but further testing on this relationship is advisable. An analysis of the relationships between various predictor variables and changes in tasseled cap wetness (and thus conifer mortality) support the expectations that drier and warmer climatic conditions favor mountain pine beetle populations, leading to increased whitebark pine mortality.

Individual Variables: Inclusions and Omissions

Multicollinearity among the climate predictor variables means that caution must be used when one is looking at the inclusion or omission of individual variables in the final regression trees. Still, there is some utility in this exercise. Spring and fall temperature variables (ano_{Y-4}Oct, ano_{Y-4}Nov, and ano_{Y-3}Mar) were more prevalent in the full tree than winter temperature variables (ano_{Y-3}Feb), and no summer temperature variables were included at all. This finding yields support for the idea that cold-related mortality is the most important factor in MPB population dynamics (Régnière and Bentz 2007) and that the seasonally variable production of cryoprotectants by MPBs makes them most vulnerable to cold in late fall and early spring (Bentz and Mullins 1999).

The lack of seasonal summary terms in either the full or final tree is notable, especially considering that the tree made from only seasonal climate summaries explained nearly as much deviance (DDE = 0.1419) as the all-climate tree (DDE = 0.1483). This result might be related to field studies and mathematical models indicating that MPBs respond to phloem temperature on hourly scales, not daily or monthly, so 6- or 12-month averages will miss a lot of detail (Logan and Bentz 1999, Bentz and Schen-Langenheim 2006). EWDI responds to changes in soil/canopy moisture, so it is also interesting that no precipitation anomalies from the 10 months before the image date were included in either the full or climate tree. Only one term (avg30Dec) from the 30-year-average temperature and precipitation data sets was included in either final model. This result might indicate that, within the narrow bioclimatic band that covers whitebark pine habitat, differences from slightly warmer or cooler sites are not very important. A similar study performed on a wider range of pine forests might find that long-term climatic averages are important in stratifying the data set. The lack of inclusion of 30-year-average climate data could also be due to the spatial scale of the data (800 m), which incorporates much variation of vegetation within a single climate pixel.

An analysis of yearly subsets of the data set was not illuminating. There did not appear to be any pattern to differences in DDE between the different years. Although very different predictor variables were included in the regression trees for each of these yearly subsets, there once again did not appear to be any pattern to these differences, such as coming from different seasons or different growth years.

Extensions and Implications

A recent review article on climate change and bark beetles found a need for both "better understanding and more refined models that integrate indirect effects of climate change on host trees with bark beetle population success" (Bentz et al. 2010). The current study begins to fill this knowledge gap between mathematical models of expected MPB behavior given various climate parameters and field studies that intensively analyze temperature and MPB survival on only a few hundred individual trees. The relationships between observed biophysical data that correlate with whitebark pine mortality and climate data were dissected. The spatial patterns of conifer mortality correspond well with predicted patterns based on our model, but the match could be improved. One shortcoming was the smoothing of data in the predicted EWDI maps and the general lack of extreme values that would indicate severe MPB outbreaks. This is probably because of the much coarser scale of the climate anomaly data (4000-m pixels)

compared with the resolution of Landsat (30-m pixels) from which the EWDI values are derived. It is interesting to note that although the topographic variables (elevation, slope, and aspect) were originally at a spatial scale similar to that of EWDI, they were still not nearly as important in the predictive models as the much coarser climate data. In addition to reducing the spatial scale of the climate data, the temporal scale was also not ideal. MPBs respond to hourly changes in tree phloem temperature, so monthly average data are too coarse of a temporal scale. Future researchers could either use more temporally explicit data (such as hourly data from SNOTEL stations) or generate a pseudo-daily climate data set from monthly data using stochastic climate models (Régnière and Bolstad 1994). The regression trees created here could also be applied to forecasted future climate regimes to predict the impact of future climates on MPBs in whitebark pine habitat.

Finally, the results of this study are important to discussions of the future health of both whitebark pine and the entire high-mountain ecosystem that this keystone species supports. Middle-range climate change models predict average annual surface temperatures in the Northern Rockies to increase by 3.5°C by 2100, with higher levels of warming occurring in the winter (Christensen et al. 2007). This level of warming would probably shift MPB life cycles in GYE whitebark pine toward epidemic-sustaining univoltinism, potentially devastating the whitebark pine (Logan et al. 2010). A severe decline in whitebark pine populations would also be cause for concern for the grizzly bear. Grizzly bear food sources were considered to be secure by the delisting agency (Hall 2007), which is probably not the case if whitebark pine populations collapse due to MPB. This discrepancy was part of the rationale behind the 2010 relisting of the grizzly bear to the threatened species list (Federal Register 2010).

This study provides the first evidence inferred from Landsat data of a link between climate and whitebark pine mortality at stand-level resolution across an ecosystem. Drier and warmer climates were shown to be correlated with increased conifer mortality in whitebark pine habitat, potentially due to increased mountain pine beetle activity. These links reinforce concerns of both the future viability of whitebark pine and the mountain ecosystem it supports.

Literature Cited

AMMAN, G.D. 1973a. Population changes of the mountain pine beetle in relation to elevation. *Environ. Entomol.* 2:541–547.

AMMAN, G.D. 1973b. Temperature dependent development of the mountain pine beetle (Coleoptera: Scolytidae), and simulation of its phenology. *Can. Entomol.* 123:1083–1094.

AMMAN, G.D., M.D. MCGREGOR, AND R.E. DOLPH. 1989. *Mountain pine beetle, forest insect, and disease leaflet 2* (revised). US For. Serv., Washington, DC. 14 pp.

ARNO, S.F. 1986. Whitebark pine cone crops—A diminishing source of wildlife food? *West. J. Appl. For.* 1:92–94.

ARNO, S.F., AND R.J. HOFF. 1990. *Pinus albicaulis* Engelm. whitebark pine. P. 268–279 in *Silvics of North America,* Burns, R.M., and B.H. Honkala (eds.). US For. Serv., Washington, DC.

AUKEMA, B.H., A.L. CARROLL, Y. ZHENG, J. ZHU, K.F. RAFFA, R.D. MOORE, K. STAHL, AND S. TAYLOR. 2008. Movement of outbreak populations of mountain pine beetle: Influences of spatiotemporal patterns and climate. *Ecography* 31:348–358.

BENTZ, B., AND G. SCHEN-LANGENHEIM. 2006. The mountain pine beetle and whitebark pine waltz: Has the music changed? P. 51–60 in *Proc. of the Conference on whitebark pine: A Pacific Coast perspective; Ashland, OR*. US For. Serv. R6-NR-FHP-2007-01. Pacific Northw. Reg., Portland, OR.

BENTZ, B., AND D.E. MULLINS. 1999. Ecology of mountain pine beetle (Coleoptera: Scolytidae) cold hardening in the intermountain west. *Environ. Entomol.* 28:577–587.

BENTZ, B.J., J. RÉGNIÈRE, C.J. FETTIG, E.M. HANSEN, J.L. HAYES, J.A. HICKE, R.G. KELSEY, J.F. NEGRÓN, AND S.J. SEYBOLD. 2010. Climate change and bark beetles of the western United States and Canada: Direct and indirect effects. *Bioscience* 60:602–613.

BOCKINO, N. 2007. Disturbance interactions: Mountain pine beetle and blister rust in whitebark pine. *Castilleja* 26(1):4–6.

BROWN, J.K., S.F. ARNO, S. BARRETT, AND J. MENAKIS. 1994. Comparing the prescribed natural fire program with presettlement fires in the Selway-Bitterroot Wilderness. *Int. J. Wildland Fire* 4:157–168.

CARROLL, A., S. TAYLOR, J. RÉGNIÈRE, AND L. SAFRANYIK. 2003. Effects of climate change on range expansion by the mountain pine beetle in British Columbia, P. 223–232 in *Proc. of the mountain pine beetle symposium: Challenges and solutions*. Kelowna, British Columbia, Canada.

CARTER, G.A. 1991. Primary and secondary effects of the water content on the spectral reflectance of leaves. *Am. J. Bot.* 78: 916–924.

CHRISTENSEN, J.H., B. HEWITSON, A. BUSUIOC, X. CHEN, I. GAO, R. HELD, R.K. JONES, W.-T. KOLLI, R. KWON, V. LAPRISE, L. MAGANA RUEDA, C.G. MEARNS, J. MENENDEX, A. RAISANEN, A. RINKE, A. SARR, AND P. WHETTON (EDS.). 2007. *Regional climate projections. Climate change 2007: The physical science basis.* Contribution of Working Group I to the Fourth Assessment Report of the Intergovernmental Panel on Climate Change. Cambridge University Press, Cambridge, UK.

COHEN, W.B., AND T.A. SPIES. 1992. Estimating structural attributes of Douglas-fir/Western hemlock forest stands from Landsat and SPOT Imagery. *Remote Sens. Environ.* 41:1–17.

COLLINS, J.B., AND C.E. WOODCOCK. 1996. An assessment of several linear change detection techniques for mapping forest mortality using multitemporal Landsat TM data. *Remote Sens. Environ.* 56:66–77.

CRIST, E.P., AND R.C. CICCONE. 1984. A physically-based transformation of Thematic Mapper data—The TM tasselled cap. *IEEE Trans. Geosci. Remote Sens.* 22:256–263.

FEDERAL REGISTER. 2010. Endangered and threatened wildlife and plants; reinstatement of protections for the grizzly bear in the Greater Yellowstone ecosystem in compliance with court order. *Fed. Regis.* 75(58):14496–14498. Available online at federal register.gov/a/2010-6802; last accessed Nov. 24, 2010.

FRANKLIN, S.E., M.B. LAVIGNE, L.M. MOSKAL, M.A. WULDER, AND T.M. MCCAFFREY. 2001. Interpretation of forest harvest conditions in New Brunswick using Landsat TM enhanced wetness difference imagery (EWDI). *Can. J. Remote Sens.* 27: 118–128.

GIBSON, K., K. SKOV, S. KEGLEY, C. JORGENSEN, S. SMITH, AND J. WITCOSKY. 2008. *Mountain pine beetle impacts in high-elevation five-needle pines: Current trends and challenges.* US For. Serv. Forest Health Protection R1–08-020. 30 p.

GOETZ, W., P. MAUS, AND E. NIELSEN. 2009. *Mapping whitebark pine canopy mortality in the Greater Yellowstone area.* RSAC-0104-RPT1. Remote Sensing Application Center, Salt Lake City, UT.

GOODWIN, N.R., N.C. COOPS, M.A. WULDER, AND S. GILLANDERS. 2008. Estimation of insect infestation dynamics using a temporal sequence of Landsat data. *Remote Sens. Environ.* 112: 3680–3689.

GOOGLE INC. 2009. *Google Earth 5.0*. Available online at earth-.google.com; last accessed on Apr. 29, 2009.

HALL, H.D. 2007. Grizzly bears; Yellowstone distinct population; notice of petition findings; final rule. *Fed. Regis.* 72(60): 14866–14938.

HICKE, J., J. LOGAN, J. POWELL, AND D. OJIMA. 2006. Changing temperatures influence suitability for modeled mountain pine beetle (*Dendroctonus ponderosae*) outbreaks in the western United States. *J. Geophys. Res.* 111:1–12.

HOMER, C., C. HUANG, L. YANG, B. WYLIE, AND M. COAN. 2004. Development of a 2001 National Landcover Database for the United States. *Photogramm. Eng. Remote Sens.* 70:829–840.

HUANG, C., B. WYLIE, L. YANG, C. HOMER, AND G. ZYLSTRA. 2002. Derivation of a tasselled cap transformation based on Landsat 7 at-satellite reflectance. *Int. J. Remote Sens.* 23: 1741–1748.

HUANG, C., L. YANG, C. HOMER, B. WYLIE, J. VOGELMAN, AND T. DEFELICE. 2001. *At-satellite reflectance: A first order normalization of Landsat 7 ETM+ images*. US Department of Interior, US Geological Survey, EROS Data Center, Sioux Falls, SD.

KEANE, R.E. 2000. The importance of wilderness to whitebark pine research and management, P. 84–92 in *Proc. of Wilderness science in a time of change conference: Wilderness as a place for scientific inquiry, Missoula, MT*. US For. Serv. RMRS-P-15-VOL-5. Rocky Mount. Res. Stn., Ogden, UT.

KENDALL, K.C., AND R.E. KEANE. 2001. Whitebark pine decline: Infection, mortality, and population trends. P. 221–242 in *Whitebark pine communities: Ecology and restoration*, Tomback, D.F., S.F. Arno, and R.E. Keane (eds.). Island Press, Washington, DC.

KENDALL, K.C., D. SCHIROKAUER, E. SHANAHAN, R. WATT, D.P. REINHART, R. RENKIN, S. CAIN, AND G. GREEN. 1996. Whitebark pine health in northern Rockies National Park ecosystems: A preliminary report. *Nutcracker Notes* 7:16.

KURZ, W.A., C.C. DYMOND, G. STINSON, G.J. RAMPLEY, E.T. NEILSON, A.L. CARROLL, T. EBATA, AND L. SAFRANYIK. 2008. Mountain pine beetle and forest carbon feedback to climate change. *Nature* 452:987–990.

LANDENBURGER, L., AND R.L. LAWRENCE. 2006. Mapping whitebark pine distribution throughout the Greater Yellowstone Ecosystem, in *Proc. of the American Society of Photogrammetry and Remote Sensing annual conference*, Reno, NV.

LANDENBURGER, L., R.L. LAWRENCE, S. PODRUZNY, AND C.C. SCHWARTZ. 2008. Mapping regional distribution of a single tree species: Whitebark pine in the Greater Yellowstone Ecosystem. *Sensors.* 8:4983–4994.

LANDFIRE. 2007. *The National Map LANDFIRE: LANDFIRE Rapid Refresh fire perimeter data.* Available online at www.landfire.gov/updatedproducts_fireperimeter.php; last accessed Feb. 22, 2009.

LAWRENCE, R.L., AND A. WRIGHT. 2001. Rule-based classification systems using Classification and Regression Tree (CART) analysis. *Photogramm. Eng. Remote Sens.* 67:1137–1142.

LOGAN, J., AND B. BENTZ. 1999. Model analysis of mountain pine beetle (Coleoptera: Scolytidae) seasonality. *Environ. Entomol.* 28:925–934.

LOGAN, J., W. MACFARLANE, AND L. WILLCOX. 2009. Effective monitoring as a basis for adaptive management: A case history of mountain pine beetle in Greater Yellowstone Ecosystem whitebark pine. *For. Biogeosci. For.* 2:19–22.

LOGAN, J., AND J. POWELL. 2001. Ghost forests, global warming, and the mountain pine beetle (Coleoptera: Scolytidae). *Am. Entomol.* 47:160–173.

LOGAN, J.A., W.W. MACFARLANE, AND L. WILLCOX. 2010. Whitebark pine vulnerability to climate-driven mountain pine beetle disturbance in the Greater Yellowstone Ecosystem. *Ecol. Applic.* 20:895–902.

MATTSON, D.J., B.M. BLANCHARD, AND R.R. KNIGHT. 1992. Yellowstone grizzly bear mortality, human habituation, and whitebark pine seed crops. *J. Wildl. Manag.* 56:432–442.

MATTSON, D.J., K.C. KENDALL, AND D.P. REINHART. 2001. Whitebark pine, grizzly bears, and red squirrels. P. 121–136 in *Whitebark pine communities: Ecology and restoration,* Tomback, D.F., S.F. Arno, and R.E. Keane (eds.). Island Press, Washington, DC.

MATTSON, D.J., AND D.P. REINHART. 1997. Excavation of red squirrel middens by grizzly bears in the whitebark pine zone. *J. Appl. Ecol.* 34:926–940.

MCDONALD, G.I., AND R.J. HOFF. 2001. Blister rust: An introduced plague. P. 193–220 in *Whitebark pine communities: Ecology and restoration,* Tomback, D.F., S.F. Arno, and R.E. Keane (eds.). Island Press, Washington, DC.

PERKINS, D.L., AND D.W. ROBERTS. 2003. Predictive models of whitebark pine mortality from mountain pine beetle. *For. Ecol. Manag.* 174:495–510.

PERKINS, D.L., AND T.W. SWETNAM. 1996. A dendroecological assessment of whitebark pine in the Sawtooth-Salmon River region, Idaho. *Can. J. For. Res.* 26:2123–2133.

POCEWICZ, A.L., P. GESSLER, AND A. ROBINSON. 2004. The relationship between effective plant area index and Landsat spectral response across elevation, solar insolation, and spatial scales in a northern Idaho forest. *Can. J. For. Res.* 34:465–480.

POWELL, J., AND J. LOGAN. 2005. Insect seasonality: Circle map analysis of temperature-driven life cycles. *Theor. Popul. Biol.* 67:161–179.

POWELL, J.A., AND B.J. BENTZ. 2009. Connecting phenological predictions with population growth rates for mountain pine beetle, an outbreak insect. *Landsc. Ecol.* 24:657–672.

PRISM GROUP AND OREGON STATE UNIVERSITY. 2004. *PRISM climate data sets*. Available online at prism.oregonstate.edu; last accessed Mar. 15, 2009.

RÉGNIÈRE, J., AND B. BENTZ. 2007. Modeling cold tolerance in the mountain pine beetle, *Dendroctonus ponderosae. J. Insect Physiol.* 53:559–572.

RÉGNIÈRE, J., AND P. BOLSTAD. 1994. Statistical simulation of daily air temperature patterns in eastern North America to forecast seasonal events in insect pest management. *Environ. Entomol.* 23:1368–1380.

REINHART, D.P., R. BENNETTS, AND C.C. SCHWARTZ. 2007. *Whitebark pine monitoring in the Greater Yellowstone Ecosystem: 2006 project summary*. National Park Service, Greater Yellowstone Inventory and Monitoring Network.

ROBERTSON, C., T. NELSON, AND B. BOOTS. 2007. Mountain pine beetle dispersal: The spatial-temporal interaction of infestations. *For. Sci.* 53:395–405.

ROGAN, J., J. MILLER, D. STOW, J. FRANKLIN, L. LEVIEN, AND C. FISCHER. 2003. Land-cover change monitoring with classification trees using Landsat TM and ancillary data. *Photogramm. Eng. Remote Sens.* 69:793–804.

SAFRANYIK, L. 2004. Mountain pine beetle epidemiology in lodgepole pine, in *Proc. of the Mountain pine beetle symposium: Challenges and solutions*, Kelowna, BC, Canada. 37 p.

SAFRANYIK, L., D.M. SHRIMPTON, AND H.S. WHITNEY. 1975. An interpretation of the interaction between lodgepole pine, the mountain pine beetle, and its associated blue stain fungi in western Canada, P. 406–428 in *Management of lodgepole pine*

ecosystems, Baumgartner, D.M. (ed.). Washington State University Cooperative Extension Service, Pullman, WA.

SCHROEDER, T.A., W.B. COHEN, C. SONG, M. CANTY, AND Z. YANG. 2006. Radiometric correction of multi-temporal Landsat data for characterization of early successional forest patterns in western Oregon. *Remote Sens. Environ.* 103:16–26.

SKAKUN, R.S., M.A. WULDER, AND S.E. FRANKLIN. 2003. Sensitivity of the thematic mapper enhanced wetness difference index to detect mountain pine beetle red-attack damage. *Remote Sens. Environ.* 86:433–443.

SMAIL, T., AND W. TANKE. 2008. *Fire history polygons for region 1-1835-2007*. Available online at www.fs.fed.us/r1/gis/thematic_data/fire_history_r1_1835_2007_poly.htm; last accessed Feb. 23, 2009.

SONG, C., AND C.E. WOODCOCK. 2003. Monitoring forest succession with multitemporal Landsat images: Factors of uncertainty. *IEEE Trans. Geosci. Remote Sens.* 41:2557–2567.

SPATIAL ANALYSIS CENTER. 2005. *Fire perimeters (from 1881 to 2005) in Yellowstone National Park, Wyoming, Montana, Idaho.* Yellowstone National Park, WY.

TOMBACK, D.F. 2001. Clark's nutcracker: Agent of regeneration. P. 89–104 in *Whitebark pine communities: Ecology and restoration*, Tomback, D.F., S.F. Arno, and R.E. Keane (eds.). Island Press, Washington, DC.

TOMBACK, D.F., S.F. ARNO, AND R.E. KEANE. 2001. The compelling case for management intervention. P. 3–28 in *Whitebark pine communities: Ecology and restoration*, Tomback, D.F., S.F. Arno and R.E. Keane (eds.). Island Press, Washington, DC.

US GEOLOGICAL SURVEY. 2009. *National elevation dataset*. Available online at ned.usgs.gov; last accessed on May 5, 2009.

WARWELL, M.V., G.E. REHFELDT, AND N.L. CROOKSTON. 2006. Modeling contemporary climate profiles of whitebark pine (*Pinus albicaulis*) and predicting responses to global warming, P. 139–142 in *Proc. of the Conference on whitebark pine: A Pacific Coast perspective; Ashland, OR*. US For. Serv. R6-NR-FHP-2007-01. Pacific Northw. Reg., Portland, OR.

WEAVER, T. 1990. *Climates of subalpine pine woodlands.* US For. Serv. INT-270. Intermount. Res. Stn., Ogden, UT.

WEAVER, T. 1992. Climates where stone pines grow, a comparison, P. 85–89 in *Proc. of the International workshop on subalpine stone pines and their environment: The status of our knowledge*. St. Moritz, Switzerland.

WULDER, M.A., C.C. DYMOND, J.C. WHITE, D.G. LECKIE, AND A.L. CARROLL. 2006a. Surveying mountain pine beetle damage of forests: A review of remote sensing opportunities. *For. Ecol. Manag.* 221:27–41.

WULDER, M.A., J.C. WHITE, B. BENTZ, M.F. ALVAREZ, AND N.C. COOPS. 2006b. Estimating the probability of mountain pine beetle red-attack damage. *Remote Sens. Environ.* 101:150–166.